CrossMark

Cu²⁺ adsorption onto ion-imprinted composite hydrogels: thermodynamics and mechanism studies

Jingjing Wang[1] · Juan Li[1]

Abstract In the current study, in situ free radical polymerization was employed to prepare Cu^{2+}-imprinted composite hydrogel (Cu^{2+}-ICH). The cross-sectional morphology of the Cu^{2+}-ICH evaluated by scanning electron microscopy indicated that the copper-loaded Cu^{2+}-ICH became rougher and the pore size of the gel became smaller compared to the unloaded Cu^{2+}-ICH. The ability of the Cu^{2+}-ICH to adsorb Cu^{2+} from aqueous solutions was assessed using batch adsorption technique. The adsorption capacity increased with the initial concentration of Cu^{2+}, but decreased as the temperature rose from 298 to 318 K. Thermodynamic parameters such as Gibbs free energy (ΔG^0), enthalpy (ΔH^0), and entropy (ΔS^0) for the Cu^{2+} adsorption were evaluated. It was suggested that the adsorption process was a spontaneous, exothermic process that had positive entropy. Selectivity study indicated that ion imprinting technique resulted in excellent affinity of the Cu^{2+}-ICH toward Cu^{2+}. Finally, the adsorption mechanism was studied by Fourier transform infrared spectroscopy and X-ray photoelectron spectroscopy. The results indicated that copper adsorption was mainly through interactions with the amine and carbonyl groups.

Keywords Composite hydrogel · Adsorption · Thermodynamic parameters · Mechanism

✉ Jingjing Wang
  jjwang1@hotmail.com

[1] School of Materials Engineering, Key Laboratory for Ecological-Environment Materials of Jiangsu Province, Key Laboratory for Advanced Technology in Environmental Protection of Jiangsu Province, Yancheng Institute of Technology, Yancheng 224051, China

Introduction

The discharge of heavy metals from industries into the environment has resulted in a number of environmental problems. The heavy metals such as copper, zinc and cadmium have become a major issue throughout the world, because they have permanent toxic effects on all living organisms, as well as constituting a threat to the environment even at a low concentration. Although copper is a bioessential element, ecological impacts may be observed when copper concentrations exceed 0.2 mg/L. According to the United States Environmental Protection Agency and World Health Organization, the permissible limit of copper in drinking water is 1.3 and 2.0 mg/dm^3, respectively [1, 2]. Intake of excessively large doses of copper by man leads to severe disease such as mucosal irritation and corrosion, central nervous system irritation followed by depression, and possible necrotic changes in the liver and kidney [3, 4]. Therefore, the elimination of copper from wastewater is highly important to protect public health and health of other living organisms. Conventional wastewater treatment technologies such as chemical precipitation, lime coagulation, reverse osmosis, and solvent extraction have several disadvantages including high-energy requirements, high capital investment, and generation of secondary toxic slurries or large volumes of sludge consisting of small amounts of heavy metals [5–7].

Hence, there is a crucial need for developing a method that is not only cost-effective, but can also be easily implemented. In the past years, hydrogel adsorption has been found to be an important and effective technology for removing heavy metal ions from aqueous solutions. The main advantages of the hydrogel adsorption are easy recovery of the heavy metals, less sludge volume produced, simplicity of design, and the meeting of strict discharge specifications [8–10]. However, hydrogels prepared from either natural or synthetic sources usually exhibit poor mechanical properties [11].

The reinforcement of the mechanical properties can be achieved by the introduction of nano-sized inorganic particles into a hydrogel matrix. Silica particles, which have strong surface activity due to the hydrogen groups on the surface, can mix and react with organic polymer. Therefore, silica has been widely applied in organic and inorganic composites [12]. Generally, addition of rigid silica particles into a polymer matrix results in an increase in the strength, modulus, and thermal stability of the composite. It has been found that strong interactions or chemical bonding between the polymer components and the silica particles may provide improvement on both reinforcement and toughening [13].

In our previous study, ion imprinting technique was employed to prepare the composite hydrogel based on acrylamide and modified silica (SiO_2–NH_2). The adsorption isotherm, kinetics, selective sorption, and regeneration ability have been investigated [14]. Ion imprinting is an attractive method for the preparation of a selective sorbent. Due to the interaction between monomers and template ions, the imprinted materials possess a predetermined arrangement of ligands and tailored binding pockets, which show stronger affinity for the template ions over other structurally related ions [15].

The present work was in continuation to our previous studies. The morphology and adsorption thermodynamics of the as-synthesized ion-imprinted composite hydrogel were investigated. Meanwhile the adsorption mechanism was elucidated by Fourier transform infrared spectroscopy (FTIR) and X-ray photoelectron spectroscopy (XPS) analysis.

Experimental

Materials

Acrylamide (AM) and silica nanoparticles (10 nm in size) were purchased from Sigma-Aldrich Chemicals. N,N'-Methylene bisacrylamide (MBA) and ammonium persulfate (APS), used as a cross-linking agent and an initiator, were purchased from Sigma-Aldrich Chemicals and used without further purification. Copper nitrate [$Cu(NO_3)_2 \cdot 3H_2O$] used in sorption experiments was purchased from Shanghai Chemical Reagents Co., China.

Preparation of Cu^{2+}-imprinted composite hydrogel (Cu^{2+}-ICH)

The Cu^{2+}-imprinted composite hydrogel (Cu^{2+}-ICH) was prepared according to our previous report [14]. Briefly, a mixture of 2.25 g of AM, 0.75 g of SiO_2–NH_2, and 0.66 g of $Cu(NO_3)_2 \cdot 3H_2O$ was added into distilled water, and the mixture was stirred vigorously for 1 h. Then 0.113 g of MBA and 0.023 g of APS were added into the solution as the cross-linker and initiator, respectively. The solution was heated for 24 h at 65 °C until the monomer AM polymerized completely. Then the product was treated with 1.0 mol/L HCl to completely leach Cu^{2+}. At last, the composite hydrogel was washed with distilled water ill neutralization and dried at 60 °C under vacuum, resulting in the desired Cu^{2+}-ICH.

In contrast, the non-imprinted composite hydrogel (NICH) was similarly synthesized in the absence of $Cu(NO_3)_2 \cdot 3H_2O$.

Adsorption capability study

Adsorption study was carried out in cylindrical glass vessels. The sample (0.1 g) was added into heavy metal ion solutions to determine the adsorption capacity under non-competitive conditions. The mixture was shaken in an orbital shaker at a speed of 150 rpm. A digital pH meter was used for pH measurements, and the pH of solutions was adjusted using the following buffer solutions: sodium acetate/hydrochloric acid for pH 2–3 and sodium acetate/acetic acid for pH 4–5. The pH of the metal feed solutions was adjusted before hydrogels were applied for the adsorption process.

The amount of the residual Cu^{2+} in the solution was determined using a Thermo Elemental-X Series inductively coupled plasma-mass spectrometer (ICP-MS) after 24 h. The amount of adsorbed metal ion (q, mmol/g) was calculated from the following equation:

$$q = \frac{(C_0 - C)V}{m},$$

where C_0 (mmol/L) and C (mmol/L) were the metal ion concentrations in the initial solution and after the adsorption for different periods of time, respectively. V (L) was the volume of the solution added and m (g) the amount of sample used.

Selective sorption study

Selective sorption study was carried out by a dynamic procedure. The imprinted and non-imprinted composite hydrogels were, respectively, used as a column-filling material for dynamic extraction of metal ions. Hydrogels were poured into a glass column, and solutions containing Cu^{2+}, Pb^{2+}, Cd^{2+}, and Ni^{2+} with a concentration of 0.005 mol/L for each kind of metal ion were passed through the column. Then the metal ions retained on the column were eluted with 1.0 mol/L HCl solutions. The concentration of the eluted metal ions was determined by ICP-MS.

Results and discussion

Preparation of Cu^{2+}-imprinted composite hydrogel (Cu^{2+}-ICH)

One of the most established procedures for the preparation of effective ion-imprinted polymers is trapping of non-polymerizable ligand in polymeric matrices. According to this method, the ion-imprinted polymeric materials containing metal ion recognition sites are synthesized via cross-linking polymerization in the presence of at least one imprint metal ion in the form of complex with a suitable ligand [16]. In the present work, template ion Cu^{2+} firstly coordinated to the $-NH_2$ from acrylamide (AAm) and modified silica (SiO_2-NH_2). Then the Cu^{2+}-ICH was synthesized by thermal-initiated free radical polymerization of the complex $Cu^{2+}-$AAm with MBA as a cross-linker in the presence of Cu^{2+}-(SiO_2-NH_2). Finally, the product was stirred in 1.0 mol/L HCl solutions and then filtered. The process was repeated until no Cu^{2+} in the filtrate was detected by ICP-MS, leaving behind some specific binding sites with functional groups in a predetermined orientation and cavities with special size of templates.

Morphology study

The cross-sectional morphology of the Cu^{2+}-ICH before and after Cu^{2+} adsorption was evaluated by scanning electron microscopy (SEM). Figure 1 shows that the Cu^{2+}-ICH exhibited three-dimensional porous structure before adsorption, while the copper-loaded Cu^{2+}-ICH became rougher and the pore size became smaller, which suggested the uniform distribution of Cu^{2+} on the sorbent. The results indicated that the Cu^{2+} binding exerted fundamental effect on the morphological feature of the adsorbent. Similar results were found in the previous reports, such as Pb^{2+} adsorption onto ion-imprinted poly(vinylimidazole)–silica hybrid copolymers [17],
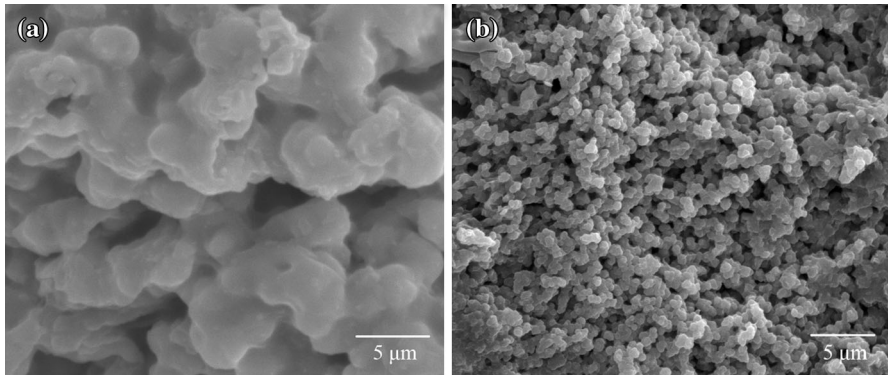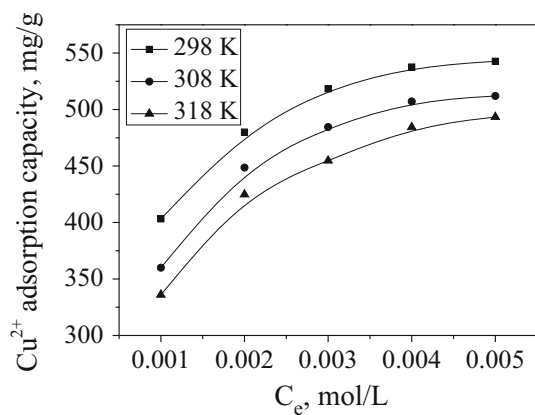
Fig. 1 SEM photographs of **a** Cu^{2+}-ICH and **b** Cu^{2+}-ICH with Cu^{2+} adsorption (magnitude: 5000×)

Fig. 2 Effect of initial Cu^{2+} concentration on the adsorption capacity of Cu^{2+}-ICH at pH 5.0 with an adsorption time of 24 h

Hg^{2+} adsorption onto the poly (methacrylic acid)-based sorbents [18], and Cu^{2+} adsorption onto the ion-imprinted polymeric nanoparticles [19].

Adsorption behavior

The adsorption capacity of the Cu^{2+}-ICH is an important parameter to determine how much sorbent is required to quantitatively adsorb a specific amount of Cu^{2+} from aqueous solutions. According to our previous report [14], the maximum adsorption capacity was observed at pH 5.0. Therefore, an initial pH value of 5.0 was selected as the experimental condition.

As shown in Fig. 2, the adsorption capacity of the Cu^{2+}-ICH linearly increased when the initial concentration of Cu^{2+} was between 0.001and 0.005 mol/L, and reached a plateau in the adsorption profile at 0.005 mol/L. The maximum amount of Cu^{2+} adsorbed by Cu^{2+}-ICH was found to be 542.72, 512.00 and 493.38 mg/g, respectively at 298, 308, and 318 K.

According to our previous report [20], the maximum sorption capacity of the non-imprinted composite hydrogel (NICH) was 474.88 mg/g at 298 K when the initial concentration of Cu^{2+} was as high as 0.01 mol/L. It was clearly indicated that the Cu^{2+}-ICH developed in this study had a great potential for the treatment of wastewater containing Cu^{2+} from various industries.

Figure 2 also indicated that the adsorption capacity of Cu^{2+}-ICH decreased as the temperature rose from 298 to 318 K. Because adsorption is an exothermic reaction, the high temperature is disadvantageous to the adsorption process. This result was very similar to the previous work in which the adsorption capacity of carboxymethyl-chitosan was found to decrease with the increase of temperature below 328 K [21].

Adsorption thermodynamics study

As related to temperature effect, the thermodynamic parameters such as Gibbs free energy (ΔG^0), enthalpy (ΔH^0), and entropy (ΔS^0) were calculated for this adsorption system.

The Gibbs free energy change ΔG^0 could indicate the degree of the spontaneity of the adsorption process. For significant adsorption to occur, the free energy changes (ΔG^0) of adsorption must be negative. The values of the standard Gibbs free energy were estimated using the following equation:

$$\Delta G^0 = -RT \ln K,$$

where R is the universal gas constant (8.314 J mol^{-1} K^{-1}) and T is the Kelvin temperature. K is the thermodynamic equilibrium constant for the adsorption process, which was determined using the method of Wu and Yu [22] by plotting ln (q_e/C_e) versus q_e and extrapolating to zero q_e as suggested (Fig. 3).

Adsorption equilibrium constant K for varying temperatures has been used to evaluate the thermodynamic parameters of this adsorption process and all the thermodynamic parameters of the adsorption process are shown in Table 1. It was

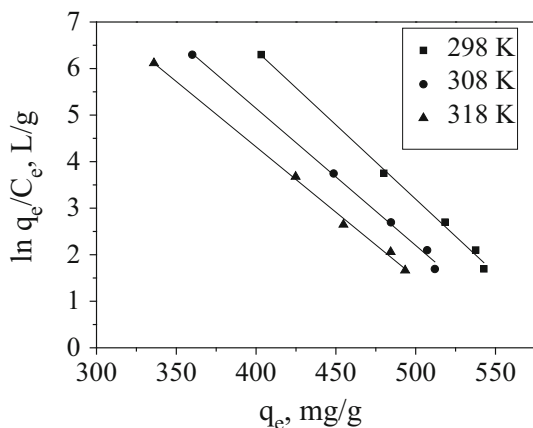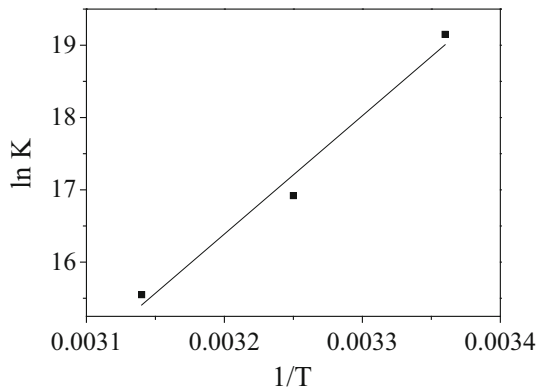**Fig. 3** Plots of ln (q_e/C_e) as a function of q_e for the adsorption of Cu^{2+} by Cu^{2+}-ICH

Table 1 Thermodynamic parameters of Cu^{2+} adsorption onto Cu^{2+}-ICH

Temperature (K)	ln K	ΔG^0 (kJ/mol)	ΔH^0 (kJ/mol)	ΔS^0 (J/mol K)
298	19.15	−47.45	−136.05	297.32
308	16.55	−42.38		304.12
318	15.55	−41.11		298.55

Fig. 4 Plot of ln K versus 1/T for the adsorption of Cu^{2+} by Cu^{2+}-ICH

clear that the equilibrium constant K decreased with increasing temperature above 298 K. This suggested that this adsorption process was exothermic [23].

The negative values of free energy change (ΔG^0) indicated that this adsorption process was spontaneous in nature, whereby no energy input from outside of the system was required. The higher negative value reflected a more energetically favorable adsorption [23]. The Gibbs free energy value at 318 K was the highest negative value than the values of other temperatures. For that reason more energetically favorable, adsorption occurred at 318 K.

The enthalpy change upon adsorption can be calculated from the following equation:

$$\ln K = \frac{-\Delta H^0}{RT} + \text{constant}.$$

Therefore, the plot of ln K vs. 1/T gave a straight line whose slope was equal to $-\Delta H^0$/R (Fig. 4). The negative value of ΔH^0 (−136.05 kJ/mol) as shown in Table 1 suggested that the adsorption was exothermic and the adsorption process was enthalpically favored.

The standard change in entropy can be calculated from the following equation:

$$\Delta S^0 = \frac{\Delta H^0 - \Delta G^0}{T}.$$

The positive values of ΔS^0 indicated the increased randomness at the composite hydrogel/solution interface during the adsorption of metal ions onto composite hydrogels and significant changes occurred in the internal structure of the adsorbent during adsorption.

Selectivity study

Selectivity study was carried out by a dynamic procedure. The equilibrium sorption of Cu^{2+} on both of the Cu^{2+}-ICH and NICH was measured in the presence of several other metals, such as Pb^{2+}, Cd^{2+}, and Ni^{2+}. Figure 5 shows the recovery result of each metal ion by the imprinted and non-imprinted composite hydrogels. It was evident that only a small amount of Pb^{2+}, Cd^{2+}, and Ni^{2+} was retained by the Cu^{2+}-ICH. That was to say, the imprinted hydrogel was favorable to separate Cu^{2+} from the coexistence of other metals. In contrast, the NICH exhibited nearly identical sorption capacity for all metal ions.

For ion-imprinted hydrogels, the imprinting metal ions were removed after polymerization, leaving cavities or ''imprinted sites'' in the hydrogels, which were complementary in shape and size of the imprinting metal ions. Therefore, the resultant imprinted hydrogels could be used as extractants for selective separation and enrichment of imprinting metal ions from dilute aqueous solutions by batch or column experiments.

FTIR spectra study

Fourier transform infrared spectroscopy spectra are a useful tool to identify the presence of certain functional groups in a molecule, as each specific chemical bond often has a unique energy absorption band [24]. To understand the nature of copper adsorption and identify the possible sites of copper binding to Cu^{2+}-ICH, FTIR spectra were obtained for Cu^{2+}-ICH before and after copper adsorption. As shown in Fig. 6, the strong absorption band at the wavenumber of 3414 and 1616 cm^{-1} was characteristic of the N–H and C=O stretching vibration. The absorbance at

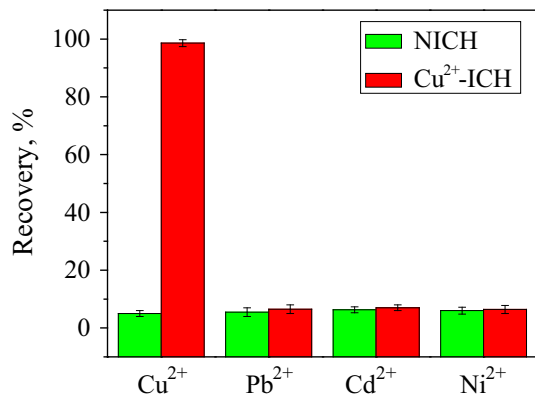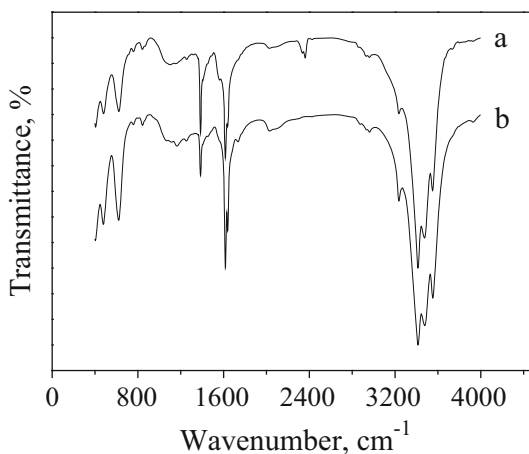Fig. 5 Recovery of metal ions by Cu^{2+}-ICH and NICH

Fig. 6 FTIR spectra of *a* Cu^{2+}-ICH and *b* Cu^{2+}-ICH with Cu^{2+} adsorption

1385 cm^{-1} was associated with the C–N stretching. The absorption peaks at wavenumber of 838 and 1099 cm^{-1} could be assigned to the presence of the Si–C and Si–O groups, respectively [25]. After the copper sorption onto Cu^{2+}-ICH, the respective vibration intensity of the N–H, C–N, and C=O groups at 3414, 1385, and 1616 cm^{-1} weakened significantly.

Copper adsorption was found to affect all of the bonds with N and O atoms, indicating that N and O atoms were the main adsorption sites for copper adsorption [26]. The major change in the transmittance for the other adsorption peaks was not obvious. For example, the absorption peaks at wavenumber of 621, 838, and 1099 cm^{-1}, which were ascribed to the C–H, Si–C, and Si–O groups, respectively, showed little difference before and after adsorption. According to the observed changes in FTIR spectra of the free and copper-loaded hydrogel, it seemed that –NH$_2$ and C=O groups were involved in the Cu^{2+} adsorption.

XPS spectra study

X-ray photoelectron spectroscopy spectra are widely used to distinguish the different forms of the same element and to identify the existence of a particular element in a material [27]. Figure 7 shows the wide-scan results of XPS spectra for the Cu^{2+}-ICH before and after copper adsorption. A small peak around binding energy (BE) of 934 eV after the copper sorption clearly indicated the accumulation of copper on the sorbent.

The high-resolution XPS spectra of N 1s are shown in Fig. 8a, b. The deconvoluted N 1s spectrum of the Cu^{2+}-ICH is shown in Fig. 8a and comprised two peaks with BEs of 394.4 and 396.3 eV. The peak at 394.4 eV was attributed to the N atom in the R–NH$_2$ group. The peak at 396.3 eV was assigned to a high oxidation state of nitrogen with positive charges (R–NH$_3^+$). After the copper sorption, the BEs of the two peaks of N 1s shifted to 395.3 and 397.1 eV, respectively, as shown in Fig. 8b. This was likely
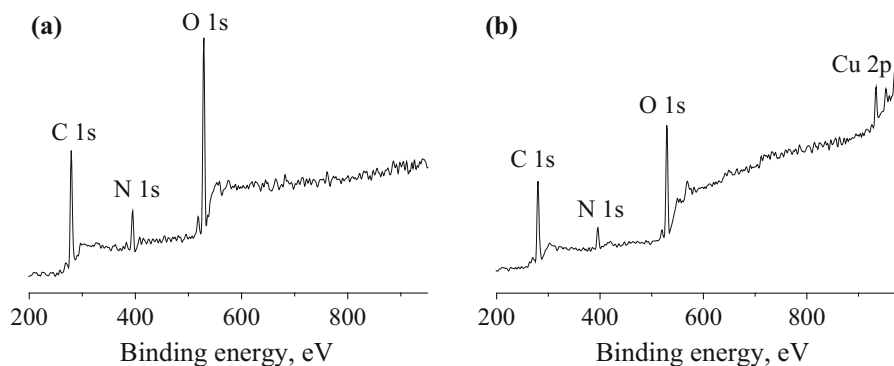
(a)

O 1s

C 1s

N 1s

(b)

Cu 2p

O 1s

C 1s

N 1s

200   400   600   800

Binding energy, eV

200   400   600   800

Binding energy, eV

Fig. 7 XPS wide-scan spectra of **a** Cu^{2+}-ICH and **b** copper-loaded Cu^{2+}-ICH

due to the formation of R–NH$_2$Cu^{2+} complexes as shown in Eqs. (1) and (2) [21]. A lone pair of electrons in the nitrogen atom was donated to the covalent bond between N and Cu^{2+}. As a consequence, the electron cloud density of the nitrogen atom was reduced, resulting in a higher BE peak.

$$R-NH_2 + Cu^{2+} \rightarrow R-NH_2Cu^{2+}, \tag{1}$$

$$R-NH_3 + Cu^{2+} \rightarrow R-NH_2Cu^{2+} + H^+. \tag{2}$$
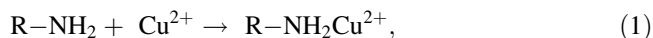
The deconvolution of C 1s spectra in Fig. 8c produced three peaks with BE of 277.5, 279.1, and 282.0 eV, respectively. These peaks could be assigned to the C atom in forms of C–C, C=O, and C–N. The carbon atoms in these three respective organic functional groups were typical in Cu^{2+}-ICH and had different electron density. After copper adsorption, the binding energy of C=O and C–N shifted to 279.8 and 283.2 eV, respectively, as shown in Fig. 8d. It indicated that C=O and C–N groups were involved in the Cu^{2+} sorption, in which oxygen and nitrogen atoms donated electrons to Cu^{2+} and thus the electron density at the adjacent carbon atom in C=O and C–N decreased [21].

In addition, the O 1s spectra could be deconvoluted into only a single peak, as shown in Fig. 8e. The peak at the binding energy of 528.9 eV could be assigned to the oxygen atom in the form of C=O groups. Figure 8f showed that the binding energy of the peak for the copper-loaded sorbent had a certain degree of shift, which was due to the copper ions bound onto the oxygen atoms and thus the electron density toward the oxygen atoms was decreased. The changes in the BE of C=O indicated that the C=O group was involved in the sorption of copper, which was consonant with the observations in C 1s analysis.

Conclusions

In the present study, Cu^{2+}-imprinted composite hydrogel (Cu^{2+}-ICH) has been prepared by in situ free radical polymerization. The morphology study indicated that the Cu^{2+}-ICH exhibited flat and smooth surface, while after Cu^{2+} adsorption Cu^{2+}-
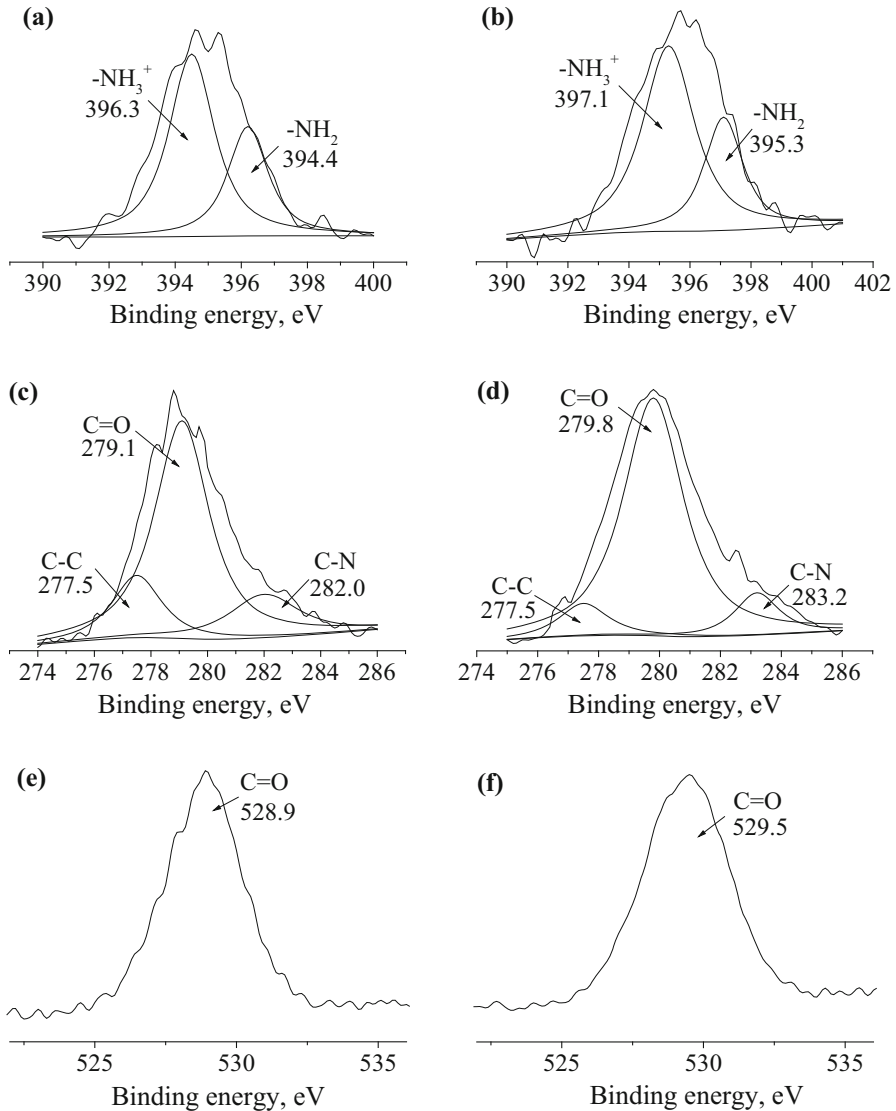
Fig. 8 XPS spectra of **a** N 1s of Cu²⁺-ICH; **b** N 1s of copper-loaded Cu²⁺-ICH; **c** C 1s of Cu²⁺-ICH; **d** C 1 of copper-loaded Cu²⁺-ICH; **e** O 1s of Cu²⁺-ICH; **f** O 1s of copper-loaded Cu²⁺-ICH

ICH presented a rough surface. The Cu²⁺ sorption on Cu²⁺-ICH was temperature dependent, and the adsorption capacity decreased as the temperature rose from 298 to 318 K. The results of the thermodynamic study indicated that the metal ion adsorption was a spontaneous and exothermic process that had positive entropy. FTIR and XPS spectra showed that amine and carbonyl groups were involved in the sorption of copper. The ion-imprinted composite hydrogel was favorable to separate

Cu^{2+} from the coexistence of other metals. In contrast, the non-imprinted composite hydrogel exhibited nearly identical sorption capacity for all metal ions.

References

1. Anirudhan TS, Suchithra PS (2010) Heavy metals uptake from aqueous solutions and industrial wastewaters by humic acid-immobilized polymer/bentonite composite: kinetics and equilibrium modeling. Chem Eng J 156:146–156
2. Chen JH, Liu QL, Hu SR, Ni JC, He YS (2011) Adsorption mechanism of Cu(II) ions from aqueous solution by glutaraldehyde crosslinked humic acid-immobilized sodium alginate porous membrane adsorbent. Chem Eng J 173:511–519
3. Yao ZY, Qi JH, Wang LH (2010) Equilibrium, kinetic and thermodynamic studies on the biosorption of Cu(II) onto chestnut shell. J Hazard Mater 174:137–143
4. Ozsoy HD, Kumbur H, Saha B, van Leeuwen JH (2008) Use of *Rhizopus oligosporus* produced from food processing wastewater as a biosorbent for Cu(II) ions removal from the aqueous solutions. Bioresour Technol 99:4943–4948
5. Ucun H, Aksakal O, Yildiz E (2009) Copper(II) and zinc(II) biosorption on *Pinus sylvestris* L. J Hazard Mater 161:1040–1045
6. Karthikeyan S, Balasubramanian R, Iyer CSP (2007) Evaluation of the marine algae *Ulva fasciata* and *Sargassum* sp. for the biosorption of Cu(II) from aqueous solutions. Bioresour Technol 98:452–455
7. Amarasinghe BMWPK, Williams RA (2007) Tea waste as a low cost adsorbent for the removal of Cu and Pb from wastewater. Chem Eng J 132:299–309
8. Pourjavadi A, Amini-Fazl MS (2007) Optimized synthesis of carrageenan-graft-poly(sodium acrylate) superabsorbent hydrogel using the Taguchi method and investigation of its metal ion absorption. Polym Int 56:283–289
9. Wang J, Liu F, Wei J (2011) Enhanced adsorption properties of interpenetrating polymer network hydrogels for heavy metal ion removal. Polym Bull 67:1709–1720
10. Jeria-Orell M, Pizarro GDC, Marambio OG, Geckeler KE (2009) Novel hydrogels based on itaconic acid and citraconic acid: synthesis, metal ion binding, and swelling behavior. J Appl Polym Sci 113:104–111
11. Essawy HA, Ibrahim HS (2004) Synthesis and characterization of poly(vinylpyrrolidone-*co*-methylacrylate) hydrogel for removal and recovery of heavy metal ions from wastewater. React Funct Polym 61:421–432
12. Ji X, Hampsey JE, Hu Q, He J, Yang Z, Lu Y (2003) Mesoporous silica-reinforced polymer nanocomposites. Chem Mater 15:3656–3662
13. Sanchez C, Soler-Illia GJAA, Ribot F, Lalot T, Mayer CR, Cabuil V (2001) Designed hybrid organic-inorganic nanocomposites from functional nanobuilding blocks. Chem Mater 13:3061–3083
14. Wang J, Li X (2013) Ion-imprinted composite hydrogels with excellent mechanical strength for selective and fast removal of Cu^{2+}. Ind Eng Chem Res 52:572–577
15. Ahmadi SJ, Noori-Kalkhoran O, Shirvani-Arani S (2010) Synthesis and characterization of new ion-imprinted polymer for separation and preconcentration of uranyl (UO_2^{2+}) ions. J Hazard Mater 175:193–197
16. Singh DK, Mishra S (2010) Synthesis and characterization of Hg(II)-ion-imprinted polymer: kinetic and isotherm studies. Desalination 257:177–183
17. Tarley CRT, Andrade FN, de Santana H, Zaia DAM, Beijo LA, Segatelli MG (2012) Ion-imprinted polyvinylimidazole-silica hybrid copolymer for selective extraction of Pb(II): characterization and metal adsorption kinetic and thermodynamic studies. React Funct Polym 72:83–91

18. Singh DK, Mishra S (2010) Synthesis and characterization of Hg(II)-ion-imprinted polymer: kinetic and isotherm studies. Desalination 257:177–183
19. Shamsipur M, Besharati-Seidani A (2011) Synthesis of a novel nanostructured ion-imprinted polymer for very fast and highly selective recognition of copper(II) ions in aqueous media. React Funct Polym 71:131–139
20. Wang J, Li X (2015) Synthesis of polyacrylamide/modified silica composite hydrogels for synergistic complexation of heavy metal ions. Desalin Water Treat 53:230–237
21. Sun S, Wang A (2006) Adsorption properties of carboxymethyl-chitosan and cross-linked carboxymethyl-chitosan resin with Cu(II) as template. Sep Purif Technol 49:197–204
22. Wu J, Yu HQ (2006) Biosorption of 2,4-dichlorophenol from aqueous solution by phanerochaete chrysosporium biomass: isotherms, kinetics and thermodynamics. J Hazard Mater 137:498–508
23. Aksu Z, Kabasakal E (2004) Batch adsorption of 2,4-dichlorophenoxy-acetic acid (2,4-D) from aqueous solution by granular activated carbon. Sep Purif Technol 35:223–240
24. Li Q, Chai L, Qin W (2012) Cadmium(II) adsorption on esterified spent grain: equilibrium modeling and possible mechanisms. Chem Eng J 197:173–180
25. Wang J, Li X (2010) Preparation and characterization of interpenetrating polymer network silicone hydrogels with high oxygen permeability. J Appl Polym Sci 116:2749–2757
26. Liu H, Yang F, Zheng Y, Kang J, Qu J, Chen JP (2011) Improvement of metal adsorption onto chitosan/*Sargassum* sp. composite sorbent by an innovative ion-imprint technology. Water Res 45:145–154
27. Jin L, Bai R (2002) Mechanisms of lead adsorption on chitosan/PVA hydrogel beads. Langmuir 18:9765–9770